

A Seismic Refraction and Reflexion Study of the Continent--Ocean Transition beneath the North Biscay Margin

F. Avedik, A. L. Camus, A. Ginsburg, L. Montadert, D. G. Roberts and R. B. Whitmarsh

Phil. Trans. R. Soc. Lond. A 1982 **305**, 5-25

doi: 10.1098/rsta.1982.0023

Email alerting service

Receive free email alerts when new articles cite this article - sign up in the box at the top right-hand corner of the article or click [here](#)

To subscribe to *Phil. Trans. R. Soc. Lond. A* go to: <http://rsta.royalsocietypublishing.org/subscriptions>

A seismic refraction and reflexion study of the continent–ocean transition beneath the north Biscay margin

BY F. AVEDIK†, A. L. CAMUS‡, A. GINSBURG§,¹ L. MONTADERT‡,
D. G. ROBERTS§² AND R. B. WHITMARSH§

† *Centre Océanologique de Bretagne, B.P. 337, 29273 Brest cédex, France*

‡ *Institut Français du Pétrole, Rueil-Malmaison, France*

§ *Institute of Oceanographic Sciences, Brook Road, Wormley,
Godalming, Surrey GU8 5UB, U.K.*

The structure of the northern margin of the Bay of Biscay consists of a series of tilted and rotated blocks bounded by prominent listric faults whose polarity is consistently down toward the continent–ocean boundary. These blocks formed by rifting in late Jurassic – early Cretaceous time and are now thinly covered by post-rift sediments of Aptian to Recent age.

Seismic refraction profiles were occupied on the shelf, on either side of and across the continent–ocean transition to the shelf, using PUBS and OBS with explosives and a $4 \times 1000 \text{ in}^3$ ($4 \times 16400 \text{ cm}^3$) airgun array. Two-ship expanding spread multichannel (48-trace) seismic reflexion profiles and 30 km fixed offset reflexion profiles were located along the seismic refraction profiles on either side of the transition. A two-ship 30 km fixed offset multichannel profile was located across the transition as well as a 5 km fixed offset multichannel profile extending from the ocean crust to the shelf. Conventional 48-trace single ship multichannel profiles were located along all the refraction and two-ship reflexion lines.

Interpretation of the refraction profiles has been made by using ray tracing as well as synthetic seismograms. Conventional seismic processing techniques have been used to prepare the two-ship multichannel seismic data for interpretation. The survey is believed to be the first attempt to apply two-ship multichannel seismic data to the study of the change in crustal structure of a rifted passive margin from the shelf to the ocean crust.

The results from the experiment led to the identification of a zone of transition between continental and oceanic crust about 8 km wide. The seismic refraction data show progressive thinning of the continental crust from 33 km to about 5 km close to the transition zone. However, extension values calculated in the upper crust from the rotation of fault blocks are much less (1.1–1.4) and suggest that the majority of the thinning is achieved by extensive attenuation of the lower crust.

INTRODUCTION

Theoretical models of lithospheric extension, as well as the geological consequences of such extension in the form of rifted cratonic basins and of passive continental margins, have attracted considerable recent interest. In the European area, examples of rifted cratonic basins include the North Sea (Ziegler 1978, and this symposium) and the adjacent margins of the North Atlantic Ocean. It has become clear that extension may also occur in strike-slip and convergent settings (Bally & Snelson 1980), and examples include the Western Mediterranean (Biju-Duval

¹ On leave from Tel-Aviv University, Tel-Aviv, Israel.

² Present address: BP, Britannic House, Moot Lane, London EC2Y 9BU, U.K.

et al. 1977), the Pannonian Basin (Royden & Sclater 1981) and the Great Basin (Profett 1977). The occurrence of crustal extension, expressed by rifting, in these different geological settings emphasizes that very little is known of the mechanisms producing the rifting process, including its initiation, that cause the profound changes in crustal structure revealed by attenuation and ultimately by the formation of a spreading ocean basin.

Several innovative theoretical models (McKenzie 1978; Royden *et al.* 1980; Royden & Keen 1980; Sclater & Christie 1980; Turcotte, this symposium) have proposed mechanisms for lithospheric extension and have attempted to evaluate quantitatively the mechanical and thermal consequences of each model in terms of histories of margin and basin subsidence. These models may have a potential practical value in predicting the thermal history and thus the degree of hydrocarbon maturity in sedimentary basins formed in response to a lithospheric extension (Royden & Keen 1980; Royden *et al.* 1980; Sclater & Christie 1980). However, a rigorous description of the deep crustal structure beneath a cratonic sedimentary basin or a passive continental margin that would provide sufficient data to quantify the extension in order to constrain these models has been lacking, as has a comprehensive study of the geological and thermal history of basins that have evolved in response to lithospheric extension.

In this paper, we present some of the results of a detailed seismic refraction and reflexion study of the northern or Armorican margin of the Bay of Biscay. The study examined the deep crustal structure of the rifted and attenuated continental crust and of the transition to the adjoining oceanic crust. It is believed to be the first time that such a detailed seismic description of a rifted passive margin has been obtained. A comprehensive discussion of the seismic data and their interpretation will be published elsewhere (Ginzburg *et al.*, in preparation).

REGIONAL STRUCTURE OF NORTHERN BISCAY

The continental margin in the Southwestern Approaches to the English Channel (figure 1) consists of a broad shelf, a relatively steep slope and a broad rise that merges imperceptibly with the Biscay Abyssal Plain. The shelf is underlain by the NE–SW trending Western Approaches Basin, which seems to intersect the margin. Further north, the Cornubian High separates the Western Approaches Basin from the Celtic Sea Basin (Montadert *et al.* 1979; Roberts *et al.* 1981).

Beneath the slope and rise, multichannel seismic reflexion profiles show that the margin consists of thin Tertiary and Cretaceous sediments that overlie a series of large tilted and rotated fault blocks. Rifting apparently took place in late Jurassic – early Cretaceous time in a pre-existing marine basin, and was completed by late Aptian time (Montadert *et al.* 1977, 1979). The overall tectonic style consists of tilted and rotated fault blocks whose downthrow is consistently down toward the ocean. The pattern of faults is probably *en-echelon* or anastomosing. Many of the fault blocks are bounded by listric normal faults (figure 2*a*) with throws of up to 3000 m. The listric faults flatten out with depth close to the top of a subhorizontal group of reflectors called ‘S’ (figure 2*b*). Comparison with early refraction data suggested that this reflector corresponded to the boundary between a 4.9 and 6.3 km s⁻¹ layer (Avedik & Howard 1979). De Charpal *et al.* (1978) and Montadert *et al.* (1979) interpreted the 6.3 km s⁻¹ refractor as the boundary between the upper brittle and the lower ductile continental crust. Refraction data on the shelf (Holder & Bott 1971) suggested that the Moho shoaled from 25 km beneath the shelf break to 12 km near the continent–ocean transition, where, from the available refraction data, the observed ductile crust was estimated to be only 3 km in thickness. These

SEISMIC STUDY OF NORTH BISCAY MARGIN

7

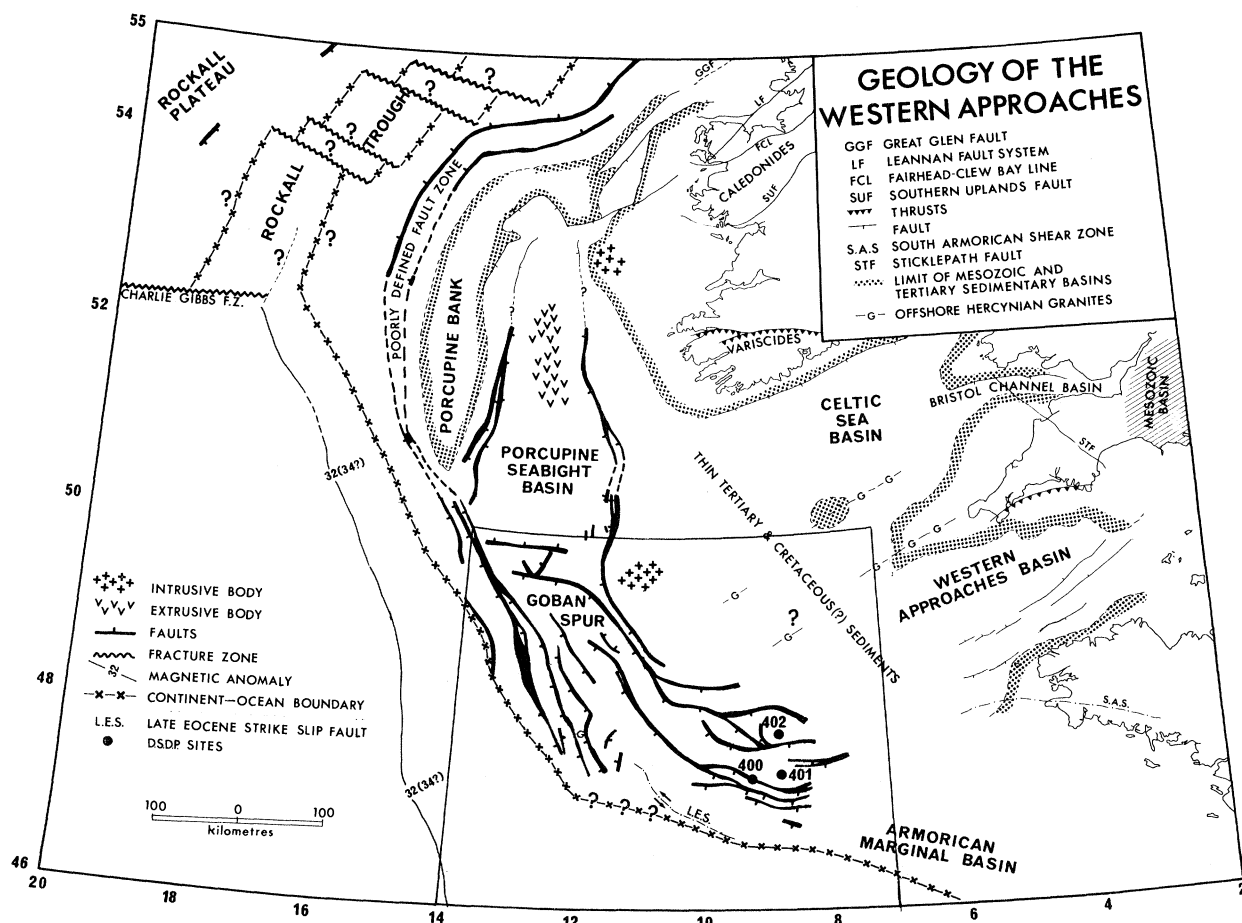
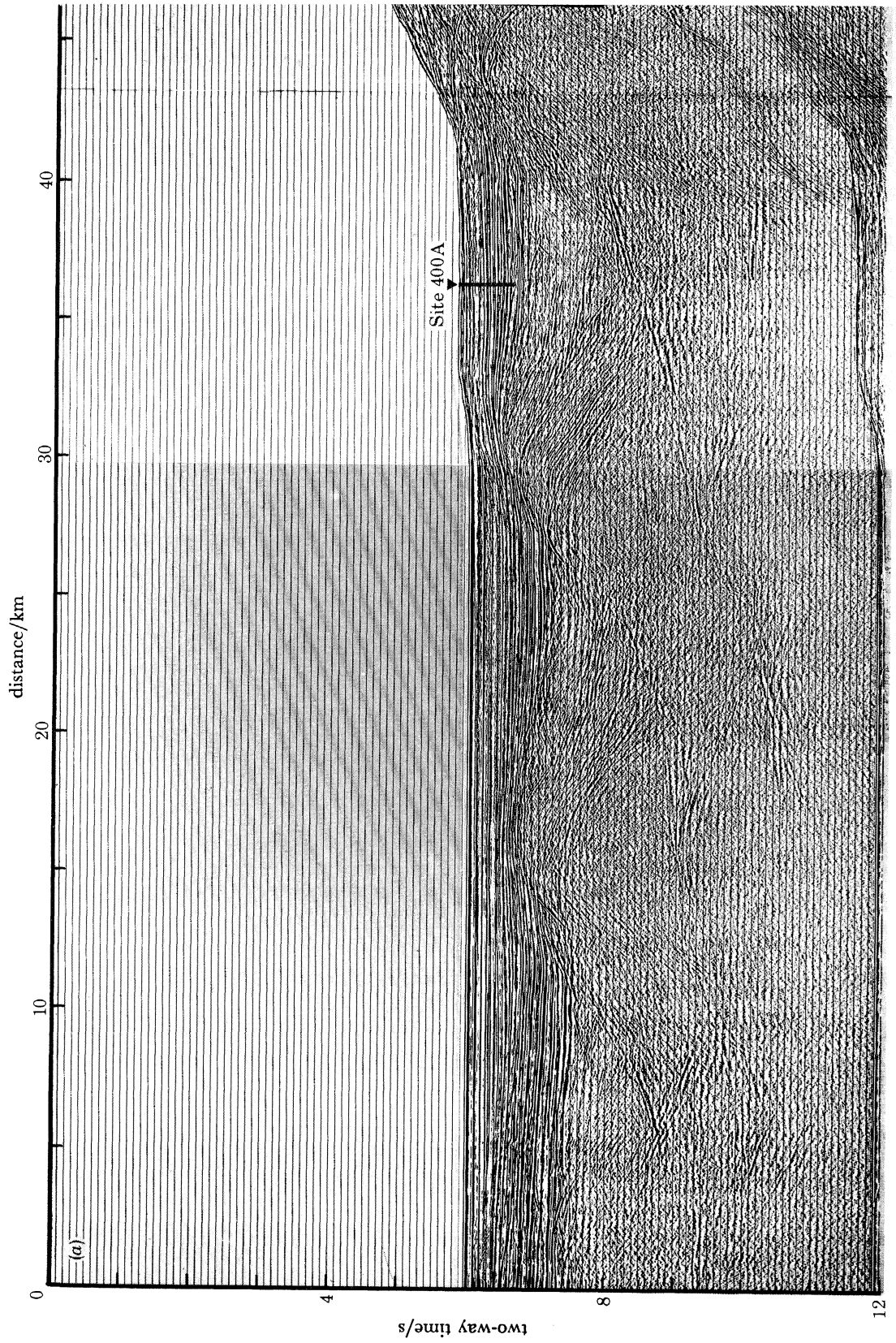


FIGURE 1. Regional structure of the continental margin of north Biscay (after Roberts *et al.* 1981).

early results showed that the observed thinning of the crust could not be fully explained by the extension of 10–15% in the upper crust and resulted in the suggestion that the lower ductile had thinned by a greater amount (de Charpal *et al.* 1978; Montadert *et al.* 1979). The drill, dredge and reflexion data suggested that at the end of rifting a system of half-graben about 2.5 km below sea level existed adjacent to the continent–ocean transition (Montadert *et al.* 1977, 1979). After rifting, regional subsidence took place in response to cooling of the lithosphere of which the continental crustal part had been thinned during the rifting process. This interpretation of attenuation, although based on good-quality multichannel seismic data, was dependent on earlier refraction profiles whose directions are now known to cross underlying fault blocks.

EXPERIMENTAL DESIGN

In June 1979, a number of single-ship refraction profiles and two-ship reflexion and refraction profiles were located on the margin. The purpose of the experiment was to define the variation in the deep structure of the continental crust from beneath the shelf, to define the continent–ocean transition and to examine the relative amounts of thinning in the upper and



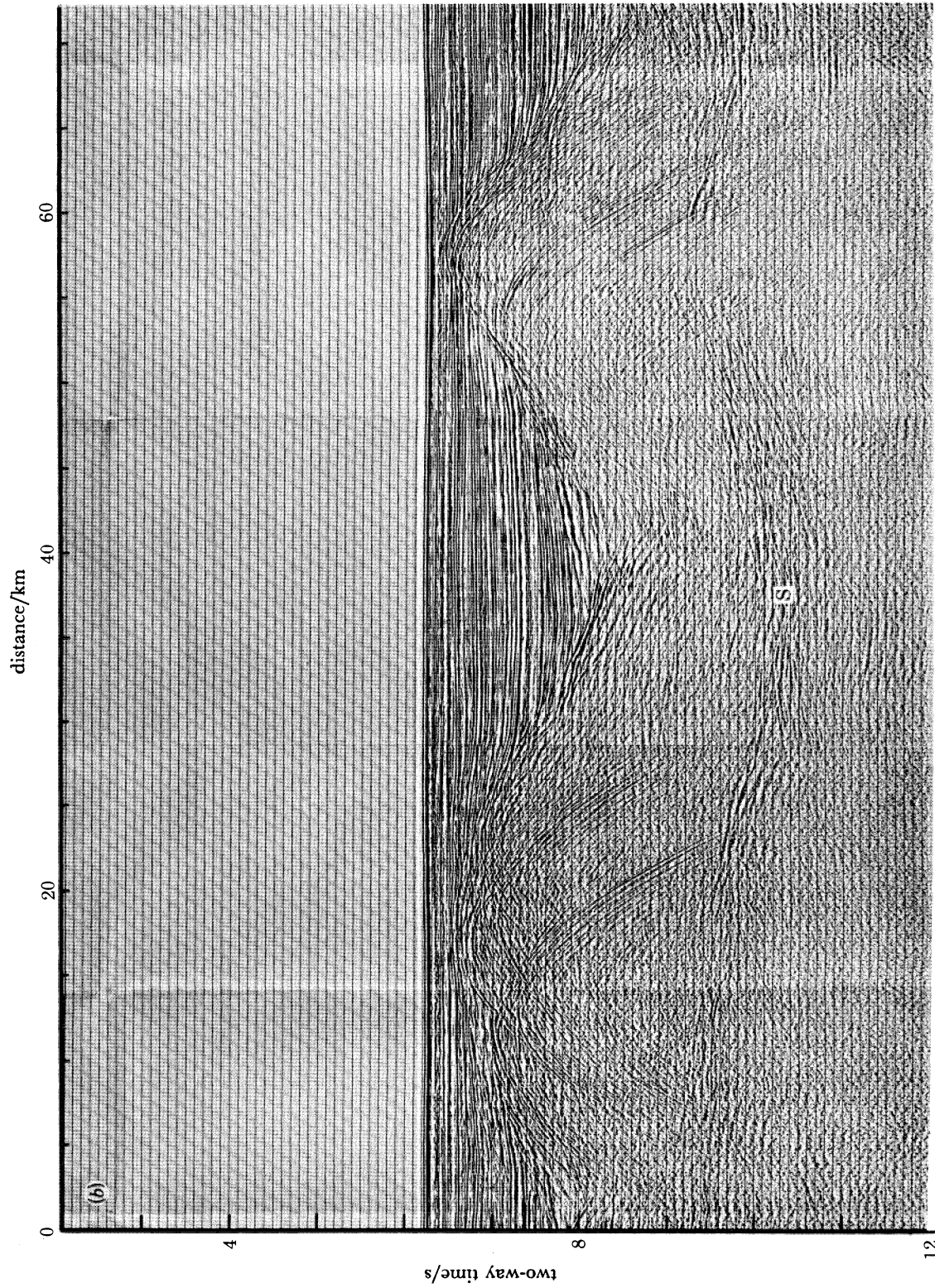


FIGURE 2. (a) An example of a series of prominent tilted and rotated fault blocks bounded by listric normal faults. The blocks contain presumed Jurassic and early Mesozoic sediments, faulted during the late Jurassic-early Cretaceous rifting episode. The position of Site 400A is shown (after Montadert *et al.* 1979). (b) Seismic profile south of Goban Spur showing the relation of the 'S' reflector' to the tilted blocks (after de Charpal *et al.* 1979).

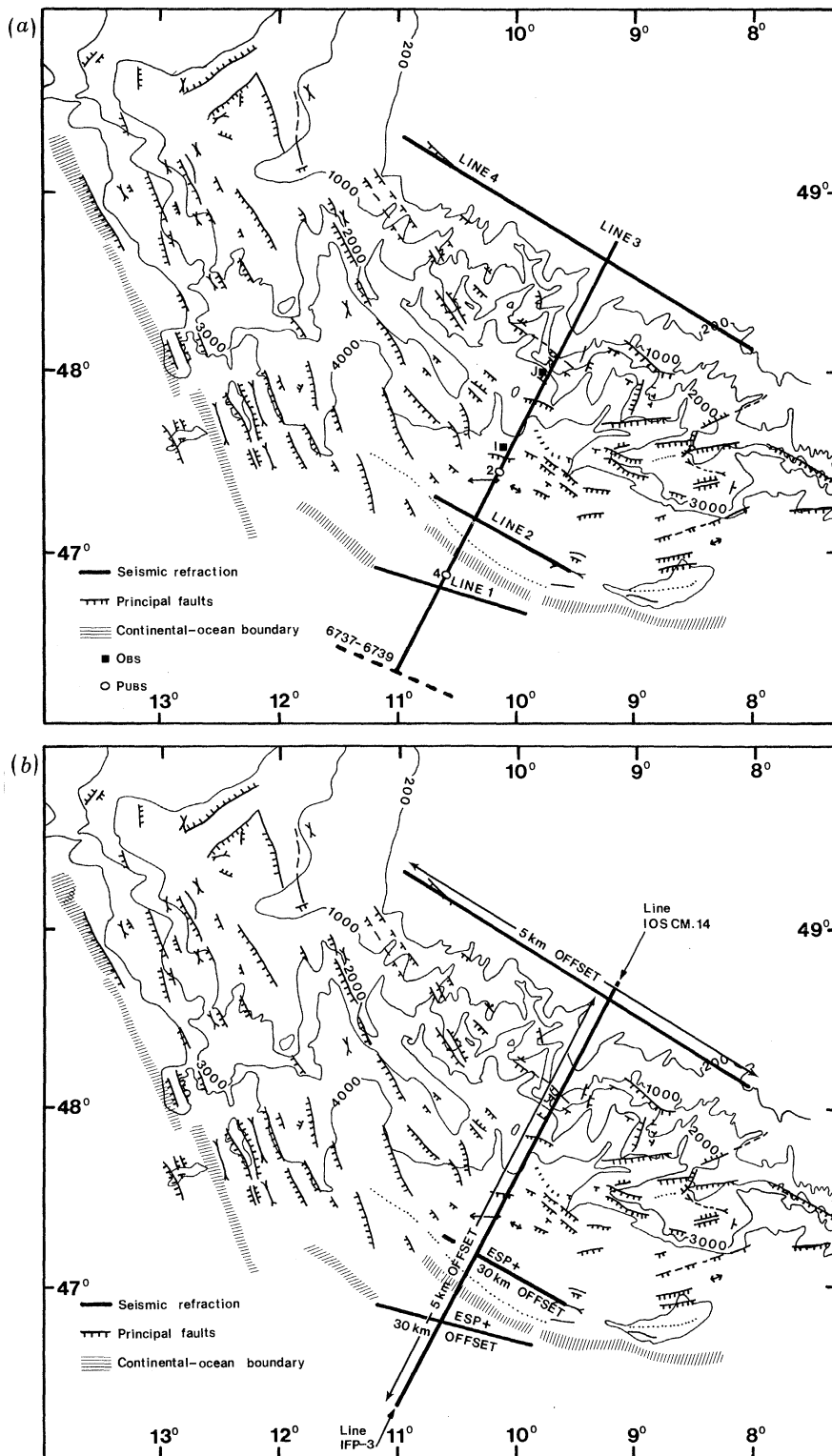


FIGURE 3. (a) Position of seismic refraction lines in relation to the major structural elements of the margin (after Montadert *et al.* 1979). I, OBS ISIS, J, OBS JULIE. (b) Position of two-ship expanding spread (e.s.p.), 30 and 5 km fixed offset profiles in relation to the major structural elements of the margin. Conventional 24-fold 48-trace multichannel single-ship profiles were occupied along all offset profiles with the exception of line 4.

lower parts of the crust. The experiment was also designed to examine the width and nature of the transition from continental to oceanic crust.

The study was carried out in two parts. During the first phase refraction profiles were shot by R.R.S. *Shackleton* using the Pop-Up Bottom Seismographs (PUBs) of the Institute of Oceanographic Sciences (Kirk *et al.* 1982) and the Ocean Bottom Seismographs (OBS) of the Centre Océanologique de Bretagne (Avedik *et al.* 1978) along the lines shown in figure 3*a*. The study area, some 30 km west of the region studied in detail around Site 400A (Montadert *et al.* 1979), was selected to avoid complications that might be posed by the prominent uplift associated with late Eocene–Oligocene shearing in the vicinity of the Trevelyan escarpment. Line 1 was situated on the oceanic crust and line 2 on the presumed thinned continental crust. As far as was possible these lines were oriented parallel to the continent–ocean transition and, for line 2, parallel to the strike of the tilted blocks. An additional unpublished reversed refraction line (figure 3*a*) situated on the ocean crust south of line 1 and made with PUBs (Discovery Station 6737–6739) was reinterpreted and incorporated in the study. Line 3 consisted of a long refraction profile from the ocean crust to the shelf encompassing the continent–ocean transition and the progressive change from attenuated crust to thick crust beneath the shelf. PUBs and OBS were deployed at various points along the line to give a series of overlapping reversed profiles. The energy source used along lines 1, 2 and 3 was a $4 \times 1000 \text{ in}^3$ ($4 \times 16\,400 \text{ cm}^3$) airgun array. Profile 4 along the shelf was unreversed and was shot by using explosive charges of up to 270 kg. It was intended to use explosives along line 3 but this was not possible for reasons beyond our control.

During the second phase of the experiment (figure 3*b*), R.R.S. *Shackleton* and the R.V. *Résolution* of the Institut Français du Pétrole occupied a series of two-ship multichannel seismic reflexion profiles. R.R.S. *Shackleton* acted as the shooting ship with a $4 \times 1000 \text{ in}^3$ airgun array, and R.V. *Résolution* acted as receiving ship with a 2.4 km 48-trace streamer. Relative positioning was maintained by using a PULSE-8 shore-based radio navigation system (accuracy $\pm 25 \text{ m}$) and radar. Shot breaks were transmitted from R.R.S. *Shackleton* to R.V. *Résolution* by using a time-break transmitter. The following types of two-ship profile were made. Along refraction lines 1 and 2 on either side of the continent–ocean transition, two-ship expanding spread profiles were made to ranges of 35 km. In addition, along both these lines and part of line 3, 30 km fixed offset profiles were made; 30 km was chosen as the offset from a preliminary Moho depth estimate to ensure that only Pn arrivals would be obtained as first arrivals. Reflexion profiles at 5 km fixed offset were also made along the whole of line 3 and line 4. Conventional 24-fold 48-trace reflexion profiles were also obtained along all refraction profiles by R.V. *Résolution*. Bathymetric and gravity data were acquired on all profiles by R.R.S. *Shackleton*.

To aid the seismic and gravity modelling, a multichannel seismic reflexion profile extending from the continental shelf to the ocean crust with a recording length of 12 s (I.O.S. line CM-14) was migrated by the Institut Français du Pétrole. We discuss below interpretation of the expanding spread (Camus 1980) and refraction data. The fixed offset data have been discussed in part by Camus (1981) and will be presented in Ginzburg *et al.* (in preparation).

EXPANDING SPREAD SEISMIC PROFILES

The principles of two-ship expanding spread seismic reflexion profiling have been discussed by Stoffa & Buhl (1979), and a detailed discussion of the way in which our data was processed can be found in Camus (1980).

In this experiment, R.R.S. *Shackleton* acted as shooting ship with a 4×1000 in³ airgun and R.V. *Résolution* as receiving ship with a 48-trace (2400 m) streamer. The time interval between shots was 80 s, resulting in a shot-receiver spacing increment of 400 m at a speed relative to the sea bed of 9.3 km h^{-1} maintained by each ship. The position of the expanding spread profiles (e.s.p.) on either side of the continent-ocean transition is shown in figure 3*b*. The recorded data were subjected to wave number and frequency filtering before sixfold stacking to ensure maximum enhancement of signal.

Interpretation of the expanding spread data has been made with reference to individual shots (48 traces per shot), as well as to the stacked section.

Individual shots in expanding spread seismic profiles

The slope(s) and intercept(s) of refracted arrivals were measured for each individual shot. This method was used to take advantage of the precision with which slopes could be measured. The multiple measurements of velocities along the line were used to assess variations in apparent velocity within a given layer. Examples of some traces displayed by using different reduction velocities are shown in figure 4.

The range of apparent velocities and intercept times are given in table 1.

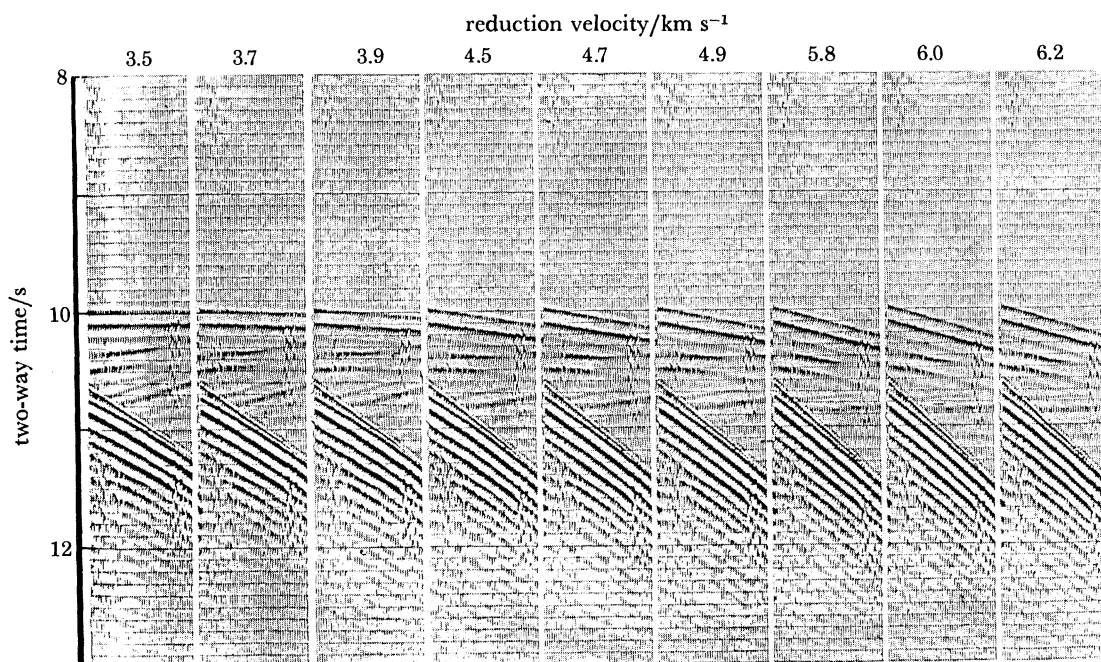


FIGURE 4. Expanding spread profile 1: examples of 48 traces per shot data displayed at different reduction velocities (from Camus 1980).

SEISMIC STUDY OF NORTH BISCAY MARGIN

TABLE 1. APPARENT VELOCITY AND INTERCEPT DATA (INDIVIDUAL SHOTS),
EXPANDING SPREAD LINES 1 AND 2

line 1 (oceanic crust)		line 2 (thinned continental crust)	
velocity/(km s ⁻¹)	intercept/s	velocity/(km s ⁻¹)	intercept/s
2.0	—	2.0	—
3.65–3.8	6.4–6.75	3.5–3.7	6.3–6.4
4.4–5.3	7.6–8.4	4.5–4.7	7.2–7.3
6.5–6.8	8.5–8.8	6.1–6.7	8.1–8.4
7.3–7.8	9–9.3	8.1–8.7	8.7–8.7

In the line 1 (ocean crust) data, the 6.5–6.8 km s⁻¹ arrivals have come from the top of the oceanic layer 3 and the 7.3–7.8 km s⁻¹ arrivals are from the Moho.

In the line 2 (thinned continental crust) data, the 4.5–4.7 km s⁻¹ velocity is a refraction from the top of the tilted blocks. The 6.1–6.7 km s⁻¹ refractor is the top of the crystalline basement within the tilted blocks, and the 8.1–8.7 km s⁻¹ refractor is the Moho.

In comparing the two lines, the scatter of the intercepts is greater on line 1 situated on the oceanic crust. Although the scatter may be due in part to the existence of strong velocity gradients within the oceanic basement, some of the scatter of velocities and intercepts on both lines probably results from the oceanic basement topography on line 1 or the tilted blocks on line 2. For example, a dip of 10° on a 8.2 km s⁻¹ refractor will reduce the apparent velocity to 7.55 km s⁻¹.

Stacked expanding spread data

Results from the expanding spread profile along line 2 are shown in figure 5*a*. Each e.s.p. was shot twice, with the two ships first approaching and then going away from each other. Intercept times were measured on both sides of the stacked sections to give averaged apparent refraction velocities and intercept times (Camus 1980).

The results calculated assuming horizontal layering are given in table 2.

TABLE 2

velocity/(km s ⁻¹)	velocity accuracy (%)	intercept/s	depth/km
line 1 (oceanic crust) from expanding spread data			
1.51	—	—	—
2.35	—	4.95	4.6
3.5	± 5	6.65	6.1
4.8	± 8	7.8	7.95
6.7	± 8	8.85	10.2
7.8	—	9.4	12.5
line 2 (thinned continental crust) from expanding spread data			
1.51	—	—	—
2.4	—	4.7	4.52
3.5	± 5	6.4	6.1
4.6	± 8	7.3	7.4
6.4	± 8	8.25	9.2
8.2	—	8.9	11.2

From these results, travel-time curves for lines 1 and 2 have been calculated and both the refracted and reflected branches are in good agreement with the observed travel-time data (figure 5*b*) (Camus 1980).

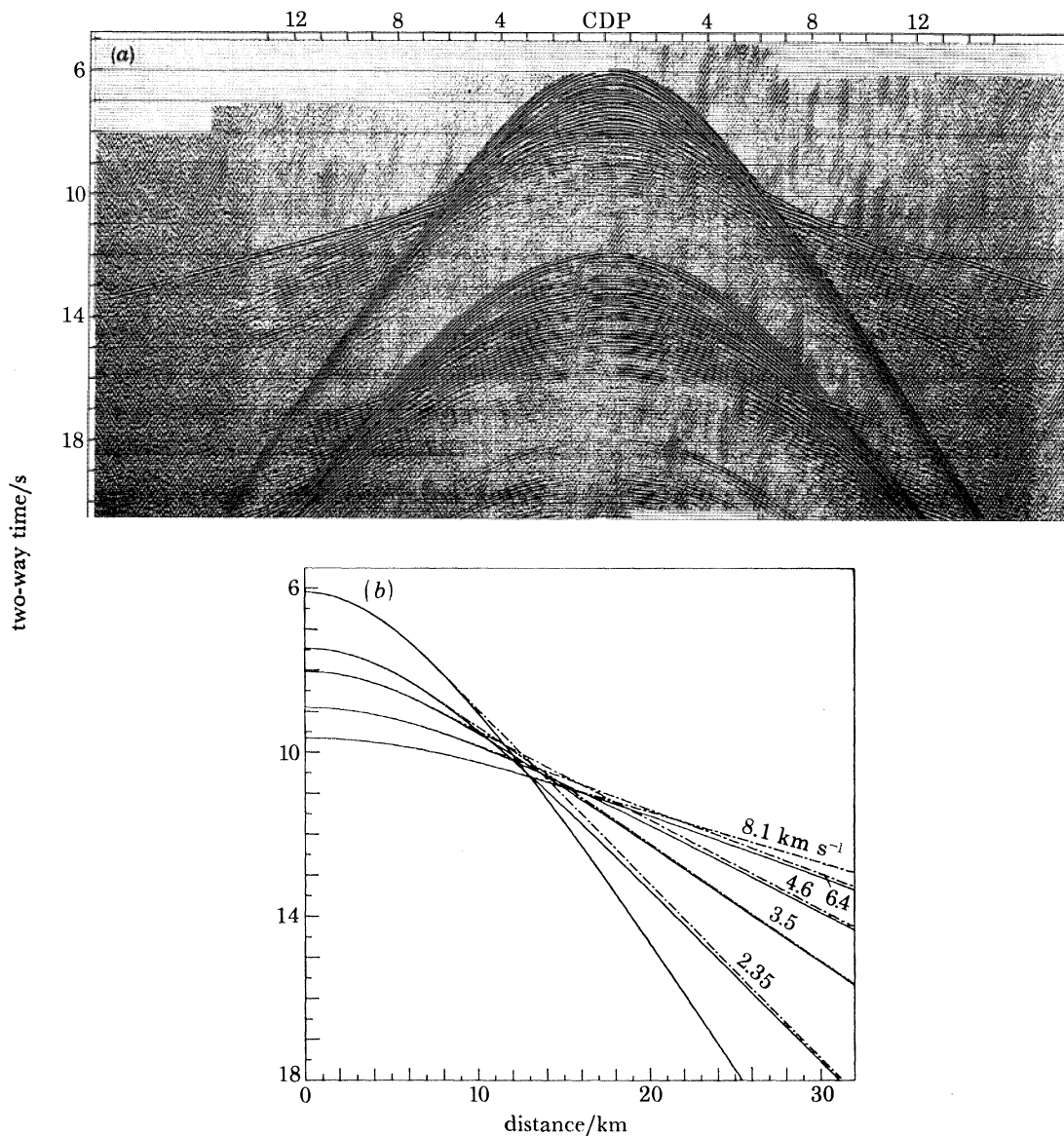


FIGURE 5. (a) Expanding spread profile 2. (b) Hodochron of expanding spread profile 2. —, Primary P-type reflections; — · —, P-type refractions.

SEISMIC REFRACTION PROFILES

Seismic refraction profiles were occupied along lines 1, 2, 3 and 4 by using PUBS and OBS. Data were recorded in analogue form in the PUBS and by pulse-coded modulation on the OBS. A 4×1000 in³ airgun array firing every 2 min at 2000 lbf in^{-2} (ca. 13.8 MPa) was used as the sound source on lines 1, 2 and 3. Line 4 was shot by using explosive charges of 11.3 kg for the near shots and 135 or 270 kg for the far shots. Ranges were computed for each trace for the PUBS data and every 15 shots for the OBS by computer modelling of water-wave travel-times. Sound velocities in the sea down to 2000 m were obtained from velocimeter data (I.O.S., unpublished data) and to greater depths from Fenner & Bucca (1971).

The PUBS data were digitized at 100 samples per second and the digitized data were plotted

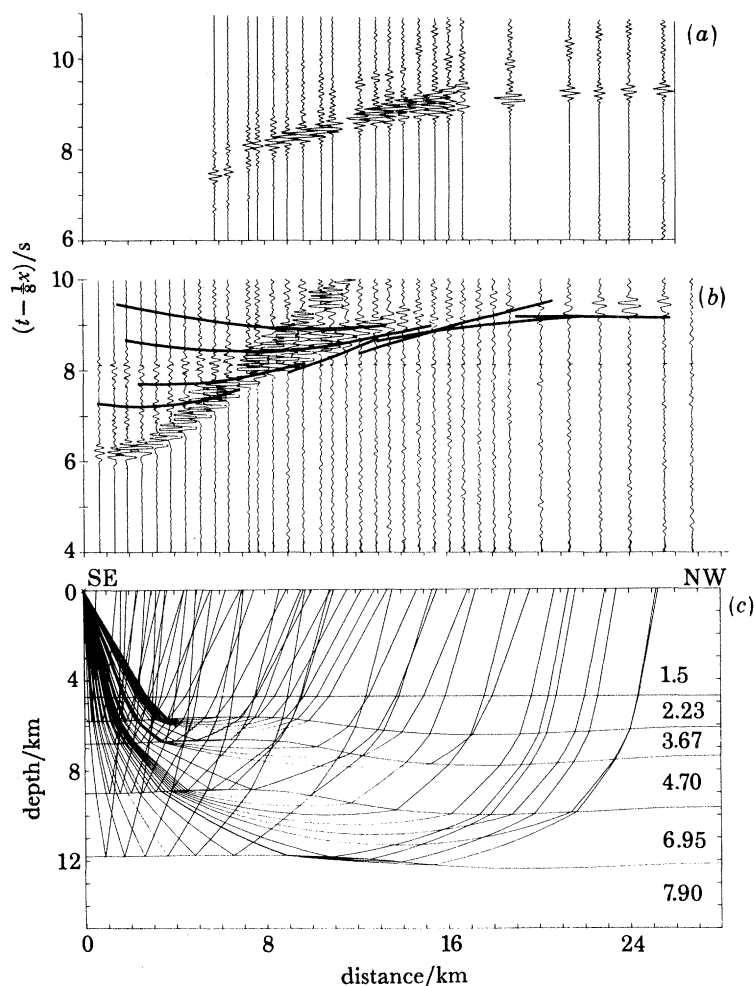


FIGURE 6. (a) Synthetic seismogram of Station 6739 (reduction velocity 8 km s^{-1}). (b) True amplitude record section (reduction velocity 8 km s^{-1}) of Station 6739 (for location see figure 3a). Hodochrons derived from the model in (c). (c) Ray trace model of the structure along reversed refraction line 6737–6739.

as filtered reduced travel-time record sections. Because of the low signal:noise ratio, particularly at ranges greater than 15 km from the PUBS, three-trace running averages were applied to the PUBS traces and the averaged sections were used for picking arrival times. The OBS data were displayed as unreduced, unaveraged variable-area record sections on which apparent velocities, but not arrival onsets, could be read with confidence.

In interpreting the data, a preliminary model was constructed based on estimates of true velocities from updip and downdip apparent velocities and from depths calculated by standard velocity intercept methods. This model was then fed into a two-dimensional ray tracing programme (Makris 1977), which was used to develop the final models. A timing correction was applied to all the arrival times to extend the ray paths to the sea surface vertically above the PUBS and OBS. The correction was based on a refraction velocity of 8 km s^{-1} . Errors in this assumption will only be significant for arrivals from the uppermost crust not studied in detail here. For Station 6739, amplitudes were modelled by using synthetic seismograms computed

by the Fuchs & Muller (1971) reflectivity method to estimate gradients within the oceanic crust (figure 6). In addition, the models were constrained by thickness and interval velocity data for the upper sedimentary layers computed from the multichannel seismic lines and, where available, from the expanding spread refraction data.

Refraction line 1 (oceanic crust)

An OBS was deployed at each end of line 1 and a PUBS in the centre. Although refracted arrivals do not persist over distances greater than 35–40 km from the OBS, a reversed refraction profile was thus obtained (figures 3*a* and 7). Calculated velocities are 2.35 and 3.32 km s⁻¹ (sediments), 4.44 km s⁻¹ (layer 2), 6.6 km s⁻¹ (layer 3) and 7.9 km s⁻¹ (upper mantle). These velocities are in good agreement with those calculated for lines 6737 and 6739, some 30 km

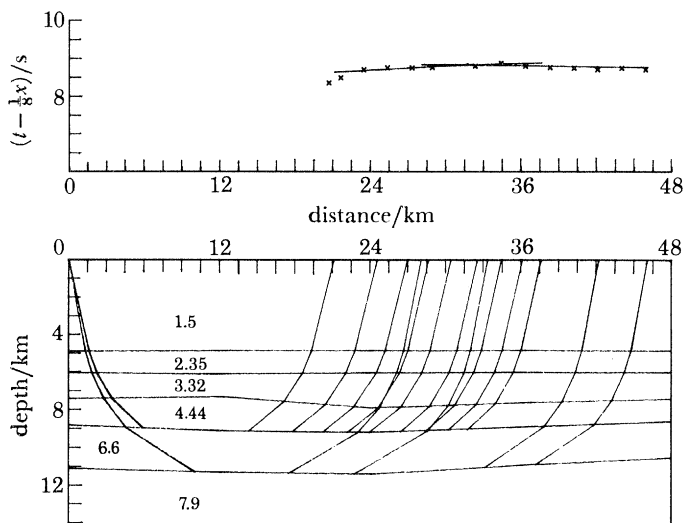


FIGURE 7. Ray trace model of refraction profile 1 (oceanic crust) obtained by using OBS and PUBS. Velocities are in kilometres per second. For location see figure 3*a*.

south of line 1. The 4.44 km s⁻¹ refractor corresponds to the 3.5 and 4.8 km s⁻¹ refractors observed on the unreversed e.s.p. line 1 (table 2). The existence of velocity gradients was deduced from the 6737 and 6739 data and is confirmed on line 1 by the concentration of energy near the 6.7–6.9 km s⁻¹ crossover distance in the PUBS data. The thicknesses of the various layers are: sediments 2.6–3.0 km, layer 2 1.6 km, layer 3 varied from 2.4 km in the west to 2 km in the east (figure 7). The model calculations were based on the arrival times and apparent velocities obtained for the PUBS data because of the poor quality of the OBS data on this line.

Refraction line 2 (thinned continental crust)

Two PUBS deployed at each end of the line (figure 3*a*) yielded record sections that have been used to calculate the model in figure 8. The velocities in this model are 3.43 km s⁻¹ for the second sediment layer, 4.52 km s⁻¹ (Palaeozoic or Mesozoic? sediments), 6.2 km s⁻¹ (crystalline basement) and 8.05 km s⁻¹ (upper mantle). The 6.2 km s⁻¹ layer is 2.5–3.0 km thick

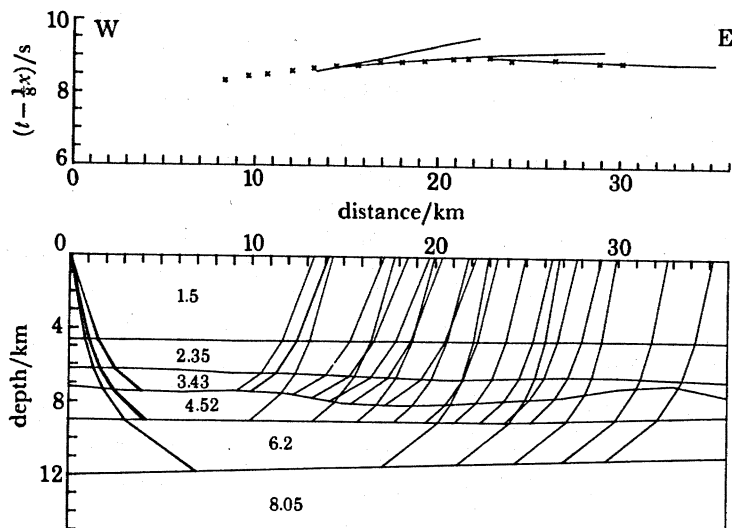


FIGURE 8. Ray trace model of refraction profile 2 (thinned continental crust) obtained by using PUBS and OBS. Velocities are in kilometres per second. For location see figure 3a.

and dips gently westward, as does the Moho. The configuration of the interfaces above the crystalline basement was obtained from the multichannel reflexion profiles.

Refraction profile 3

Refraction profile 3 (figure 3a) extends across the entire margin from the shelf to the Biscay Abyssal Plain. The profile was designed to examine the thinning of the continental crust as well as the transition from thinned continental crust to oceanic crust. The profile connects the two transverse refraction profiles discussed above, and profile 4. Three PUBS and three OBS were deployed along the line (figure 3a). Although it was originally intended to use explosive charges to obtain good arrivals at long ranges, this proved impossible and the airgun array was used perforce, thereby severely limiting the quality of the data.

The velocity structure used to constrain the refraction models at the south end of line 3 is derived from the reversed refraction profiles 1 and 2. After allowing for variations in sediment thickness obtained from multichannel seismic profiles along line 3 (lines IFP-3 and IOS CM-14, figure 3b), all variations in apparent velocity have been attributed to dip variations and not to lateral velocity variations within layers. Each reversed refraction profile between adjacent PUBS or OBS along line 3 was interpreted independently to obtain a section-by-section model for the whole line.

PUBS 4 was located on oceanic crust at the southern end of line 3 (figure 3a). The split refraction profile recorded by this PUBS covers the segment of line 3 from just south of line 2 to the Southern end of the line. The velocity distribution used in computing the model was that of line 1. The segment of the split profile south of PUBS 4 is shown in figure 9. Layer 3 apparently thins southward from 3.0 to 2.5 km.

The next segment of line 3 was recorded from PUBS 2 situated on thinned continental crust 15 km north of refraction profile 2 (figure 3a). Readable arrivals were observed to a range of 30 km to the south of PUBS 2 (figure 10). Four distinct arrivals are present and correspond to

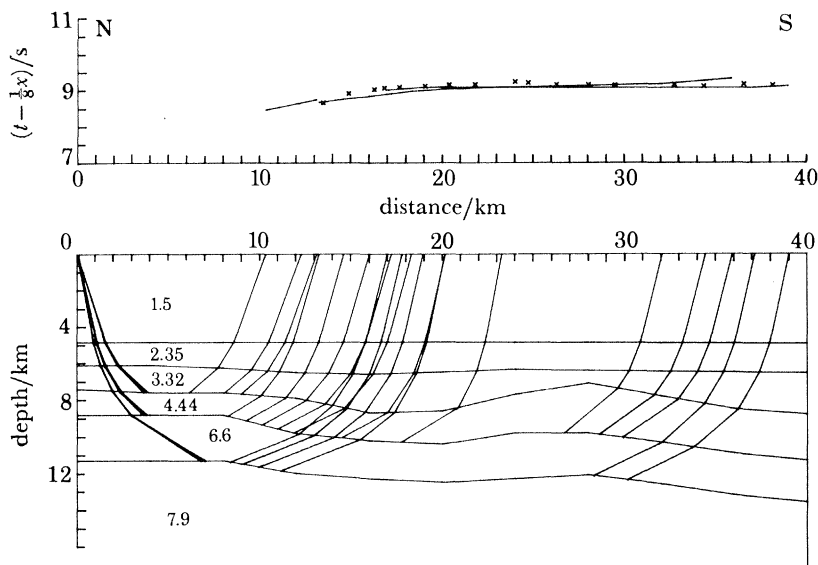


FIGURE 9. Ray trace model of reversed segment of line 3 from PUBS 4 to the south situated on oceanic crust. Velocities are in kilometres per second. For location see figure 3*a*.

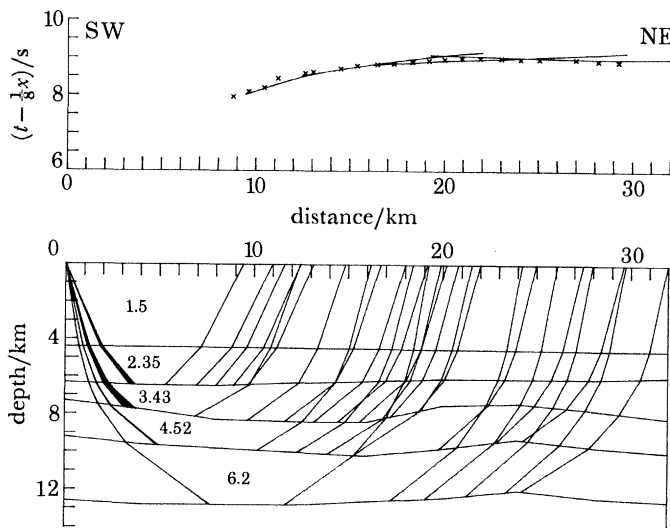


FIGURE 10. Ray trace model of reversed segment of line 3 from PUBS 2 to the south on thinned continental crust immediately north of the continent–ocean transition (cf. figure 9). Velocities are in kilometres per second. For location see figure 3*a*.

the 3.43 and 4.52 km s⁻¹ sedimentary layers, the 6.2 km s⁻¹ crystalline basement and the Moho. North of PUBS 2, however, arrivals were recorded only out to a range of 25 km and the P_n arrivals were thus not observed. However, the P_g arrivals define the configuration of the crystalline basement. The velocity distribution used in the models is derived from refraction line 2.

The results of modelling the refraction profiles from PUBS 2 and 4 provide some constraint on the position of the continent–ocean boundary. Modelling of the observations made at

PUBS 2, with the use of the velocity distribution calculated for refraction profile 2, gave good agreement between calculation and observation. However, use of the velocity distribution obtained for line 1 situated on ocean crust did not give good agreement. The converse was found in attempting to apply the results of refraction line 1 to the data obtained at PUBS 2. The discrepancy indicates that a major lateral change in crustal structure, here interpreted as the continent-ocean transition, is present within the region between PUBS 2 and PUBS 4 and probably is located between PUBS 4 and refraction profile 2 (figure 3a).

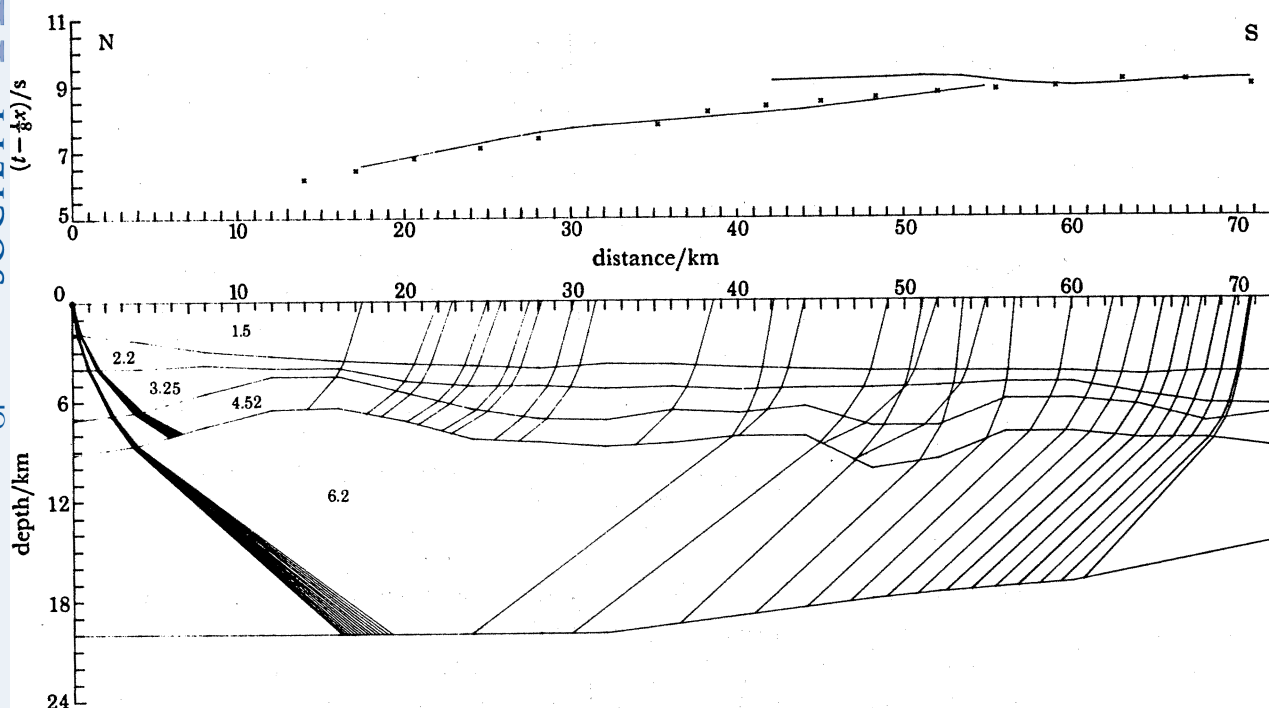


FIGURE 11. Ray trace model of reversed segment of line 3 from OBS JULIE to the southward. Note the progressive deepening of the Moho toward the continent and thickening of the crystalline crust ($V_P = 6.2 \text{ km s}^{-1}$). Velocities in kilometres per second. For location see figure 3a.

The record section south of OBS JULIE (figure 3a) has been modelled with the use of the results from PUBS 2, refraction line 2, and the multichannel reflexion profiles IFP-3 and IOS CM-14. The signal:noise ratio of the record section is low and it is fairly certain that picks at ranges over 50 km do not represent the onset of the event. None the less, the model, which is fairly well constrained by the above data, shows the progressive thickening of the crust, and particularly the lower crust, towards the shelf (figure 11). Unfortunately, because of the poor quality of the data, P^* and PIP arrivals could not be identified in the later arrivals so that the position of the discontinuity between the upper and lower crust and its behaviour in relation to the crustal thickening could not be determined.

Refraction profile 4

The refraction profile 4 (figures 3a and 12) is unreversed and was shot on the shelf across line 3 by using explosives. No reflexion data were available along this line and there is thus very little control on the depth and attitude of the sedimentary layers. However, a prominent

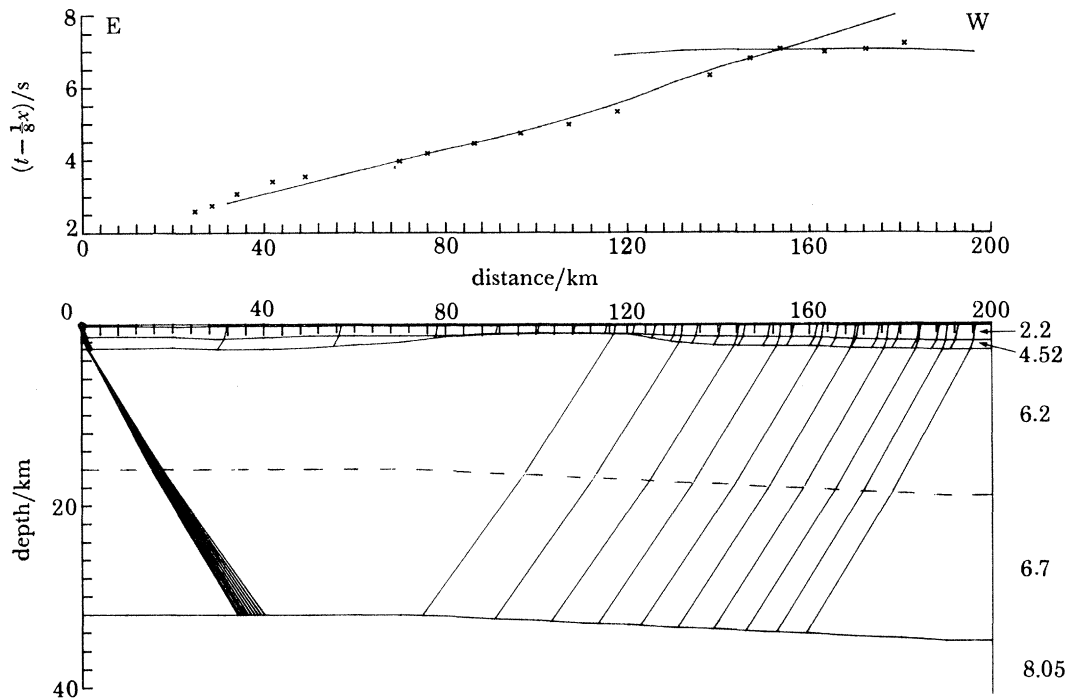


FIGURE 12. Ray trace model of unreversed line 4 shot on the shelf. Velocities in kilometres per second. For location see figure 3a.

basement high is evident from travel times. To satisfy the observed travel-time of the PmP reflexion, it has been necessary to somewhat arbitrarily divide the crust into an upper layer with a velocity gradient from 6.2 km s^{-1} at the top to 6.4 km s^{-1} at the base, and a lower crustal layer with velocities ranging from 6.4 km s^{-1} at the top to 6.7 km s^{-1} at the base.

SURVEY OF THE REFRACTION INTERPRETATION

A summary true-scale section of the distribution of the principal refracting interfaces along line 3 is shown in figure 13, together with the positions of the OBS and PUBS. Depths of the interfaces have been interpolated between OBS JULIE on line 3 and line 4 on the shelf. Uncertainties in the data are shown by dashed lines. The continent-ocean transition is inferred to lie within a narrow zone 8–10 km wide, immediately south of refraction profile 2, from the following three lines of evidence. Firstly, ray trace modelling of crustal structure south of PUBS 4 made with the use of the velocity distribution determined for the thinned continental crust along line 2 does not provide satisfactory agreement with the observed refracted arrivals. This indicates that the transition must occur north of PUBS 4 and south of refraction line 2 and PUBS 2. Secondly, the position of the transition in this region is independently suggested by the marked difference in the velocity gradients observed in the basement along lines 1 and 2. Thirdly, the refracted arrivals observed on the 30 km fixed offset profile recorded along the southern part of line 3 also show a significant change in this region. South of the inferred transition, only mantle arrivals were observed, but to the north arrivals from both basement

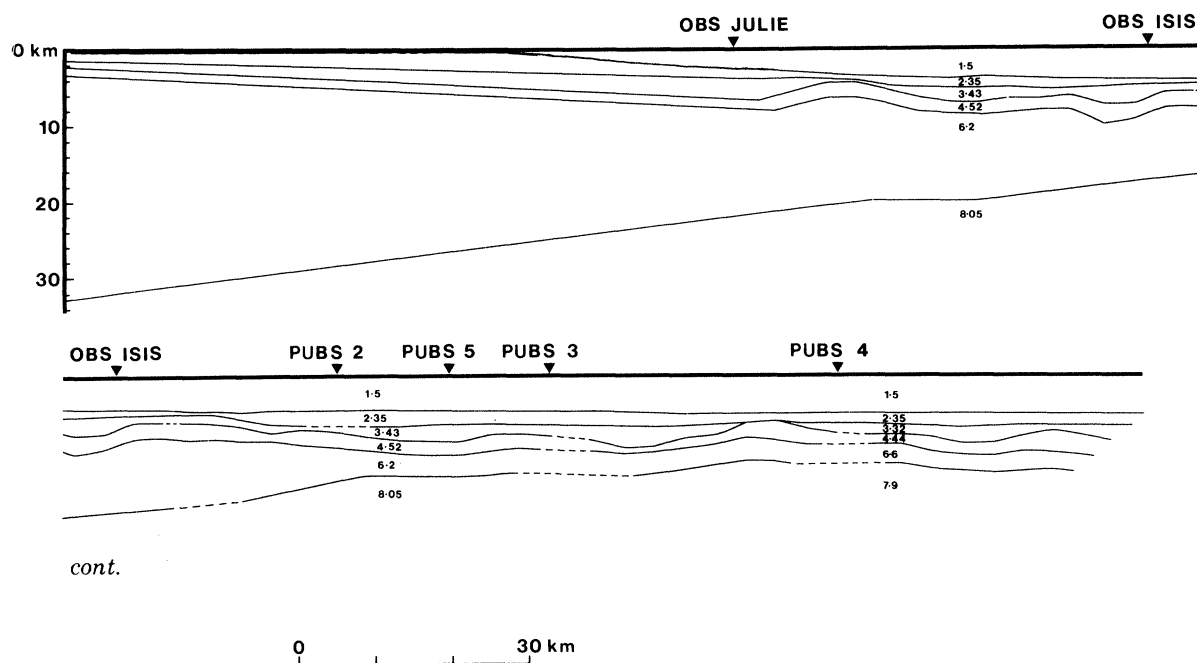


FIGURE 13. Summary true-scale section of refraction results along line 3. No vertical exaggeration. Velocities in kilometres per second. Interfaces have been interpolated between OBS JULIE and the shelf. Uncertainties are shown by dashed lines. The continent-ocean transition lies between PUBS 4 and PUBS 2. For location of section see figure 3*a*.

and mantle are present. A distinct zone of about 10 km width from which no arrivals were recorded coincides with the transition zone identified from the above data (Camus 1981).

The composite profile has a number of interesting features that will be noted here and discussed in more detail in the conclusions. Moho depths are very similar on either side of the transition, but mantle velocities are different (cf. 8.05 and 7.9 km s⁻¹). Within the continental crust, the 4.52 km s⁻¹ layer remains relatively constant in thickness in contrast to the underlying crystalline basement, which thickens from 3 to 12 km progressively toward the continent.

GRAVITY MODELS

Although the refraction data provided a very good description of the variation in crustal structure across the entire margin, the absence of information on the behaviour of the upper crust – lower crust boundary, as revealed near the foot of the slope by the ‘S reflector’ on multichannel seismic profiles, was particularly disappointing. As an alternative approach, an attempt was made to model the observed gravity profile by using the results from the refraction experiment.

Initially, density boundaries were not introduced within the continental crust in order to test the agreement between calculated and observed free-air gravity anomalies by using the refraction data alone. Interfaces were taken directly from the seismic models, and the continent-ocean boundary was positioned from the criteria discussed above. Sediment densities were picked from figures in Hamilton (1978), continental crustal densities from the Nafe-

Drake (1963) curve, oceanic crustal densities from Christensen & Salisbury (1975), and mantle densities from Christensen (1966). The model was computed by using the two-dimensional method of Talwani *et al.* (1959). The results (figure 14*a*) show a substantial discrepancy, indicating that greater mass must exist within or beneath the continental crust with respect to the oceanic crust. This excess can be accounted for by lateral density variations in the upper mantle or within the lower continental crust, or both. Further modelling showed that the

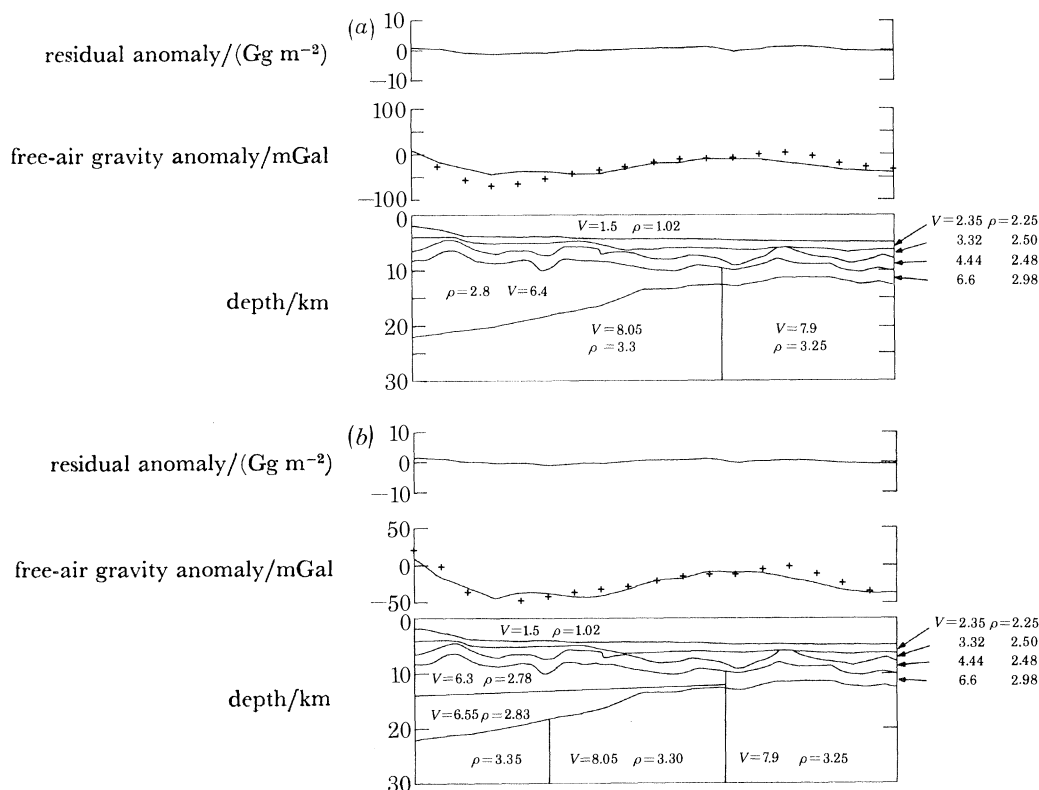


FIGURE 14. (a) Calculated (+) and observed (continuous line) free-air gravity profile along line 3. Interfaces have been taken from the summary section in figure 13, and densities from various publications (see text). The density model extended far beyond the limits of the figure and was constrained by the whole section in figure 13. The density contrasts in the upper mantle persisted to 40 km depth. (b) Calculated and observed free-air gravity profile along line 3. A density contrast in the crystalline crust at about the level of the 'S reflector' and a lateral variation in mantle density have been used to produce the agreement between calculated and observed anomaly. Otherwise the model is as in figure 13*a*. Note the thinning of the lower crust towards the continent-ocean transition. The gravity residuals can probably be explained by a lack of two-dimensionality in the real world. Note the different gravity scale with respect to (a).

required density variations in the upper mantle violate the refraction data and that more reasonable values do not fully account for the observed mass excess. A third model was computed by using a density interface within the crystalline part of the continental crust. The depth of this interface was arbitrarily chosen to correspond to the 'S reflector'. A small lateral variation in mantle density also needed to be included in the model (figure 14*b*). Agreement between calculation and observation is good. In particular, the model supports substantial oceanward thinning of the lower continental crust from 7 km to almost zero at about 100 km from the foot of the slope. Indeed, the possibility that the Moho and the base of the upper

crust (S reflector) are coincident cannot be excluded from the gravity interpretation. In marked contrast, the upper part of the crystalline continental crust remains relatively uniform in thickness between the foot of the slope and the continent–ocean transition.

DISCUSSION AND CONCLUSIONS

The results from the seismic refraction study, multichannel seismic reflection profiles and gravity modelling have been combined in the true scale section across the entire north margin of Biscay displayed in figure 15. The geometry of the fault blocks has been reconstructed from migrated seismic sections (lines IFP-13 and IOS CM-14), subsequently converted to depth by using both interval and refraction velocity data. Depths of the deeper interfaces have been taken from the refraction models. The position of the ‘S reflector’ is approximate and has been computed from interval velocity data in the sedimentary layers and the 6.2–6.4 km s⁻¹ refraction velocity in the crystalline basement.

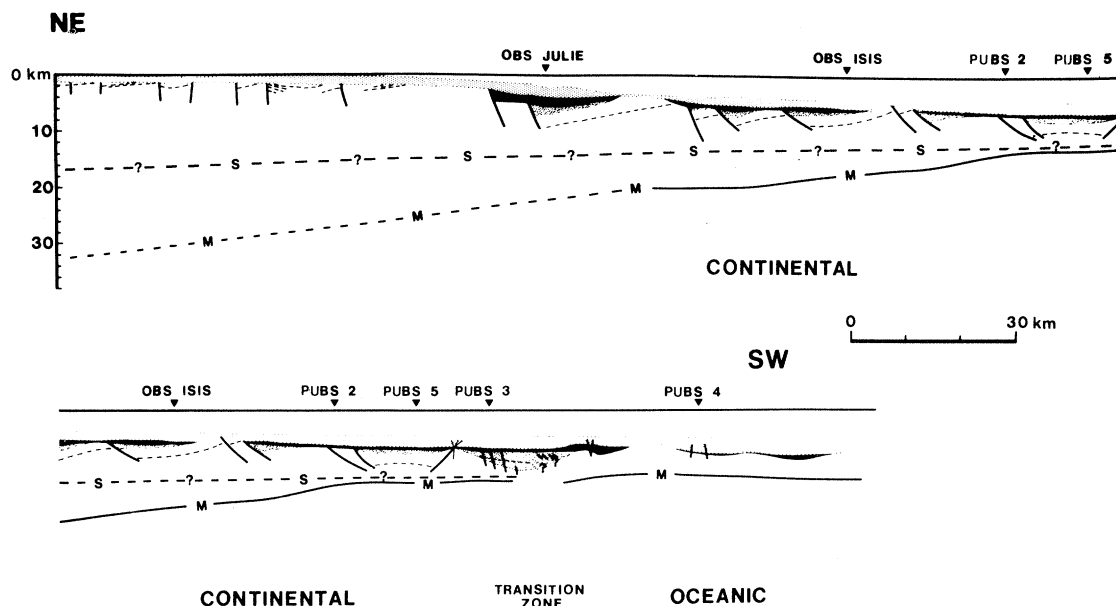


FIGURE 15. Summary section across the continental margin of north Biscay incorporating the results of the seismic refraction profile along line 3, migrated 24-fold 48-trace multichannel seismic profiles IPF-3 and IOS CM-14, and the gravity interpretation. For discussion see text.

The section has several features that have an important bearing on the problem of the measurement, as well as the mechanism, of crustal attenuation along rifted margins.

The observed position of the ‘S reflector’ indicates differential thinning within the crystalline continental crust toward the continent–ocean boundary, and the gravity model does not exclude this possibility. The lower crystalline crust thins oceanward near OBS JULIE and to a value near zero close to the continent–ocean transition. In this region, the ‘S reflector’ observed on seismic profiles may be a complex event arising from the intracrustal discontinuity and the immediately subjacent Moho. The section indicates that the larger part of the lower crust has been lost. Thinning is also evident in the upper crystalline part of the crust, but in contrast it has a global β value of between 2.5 and 3 from the shelf to the continent–ocean transition. Over

the region of extreme thinning in the lower crust, the upper crust remains relatively uniform in thickness. A third estimate of extension can be derived from the rotation of the tilted blocks. By using a true-scale section computed from the migrated multichannel seismic profile, the quantity of extension β has been found for the blocks between OBS JULIE and the continent-ocean transition. Values range between 1.1 and 1.45 and are similar to the range of values computed by Chenet *et al.* (1981) but are significantly lower than values of about 3 found for the tilted blocks by Le Pichon & Sibuet (1981; see also Foucher *et al.*, this symposium).

Estimates of the extension parameter β found by Le Pichon & Sibuet (1981) for the upper crust on the north margin of Biscay have been interpreted by them in terms of the model of uniform extension of the whole lithosphere developed by McKenzie (1978). However, the results of the refraction survey and these calculations indicate that there has been substantially greater thinning of the lower crust than of the upper. The extension parameter derived for the tilted blocks is not representative of the overall extension of the crust as was earlier noted by de Charpal *et al.* (1979) and Montadert *et al.* (1979). Indeed, according to our results, the global thinning of the crust (4.8) is much greater than that estimated by Le Pichon & Sibuet (1981).

The difference in the thinning of the upper and lower crust creates an obvious mass balance problem of some importance in extension models. One solution is to invoke rift subsidence as a consequence of a gabbro-eclogite phase transition at the Moho, as proposed by Artyushkov & Sobolev (1981). Another hypothesis is to propose that extension of the lithosphere, which perhaps had already been weakened during a previous rifting in Permo-Triassic time, began by brittle failure above and ductile failure below the 'S reflector'. As extension continued, the lower ductile part of the crust became progressively heated and gradually modified by the addition of new mantle that effectively converted the lower crust into a modified upper mantle. The lateral variation in upper mantle density implied by this hypothesis is also suggested by the best-fitting gravity model (figure 14*b*). Clearly, more work is required to assess lateral variations in the upper mantle and lower crust in the transition zone. Continued thinning by brittle and ductile flow with contemporaneous conversion of the thinned lower crust took place until the thinned upper crust rested directly on the hot upper mantle. At this stage, when the outer part of the rifted margin had subsided by rifting to about 2.0 km (Montadert *et al.* 1979), the asthenosphere might have been able to break through, thus causing the initiation of sea-floor spreading.

We acknowledge support for this study from the U.K. Department of Energy, the Natural Environment Research Council, the Centre Océanologique de Bretagne, the Institut Français du Pétrole, the Centre Nationale pour l'Exploitation des Océans and the Comité des Études Pétrolières Marins. The Masters and ships' crews of R.V. *Résolution* and R.R.S. *Shackleton* are thanked for their cooperation. The work could not have been done without the help of R. E. Kirk, J. J. Langford, P. R. Miles, S. Smith, G. Aubert, R. Conogan and R. Paron on R.R.S. *Shackleton* and M. Cassand on R.V. *Résolution*. The time-break transmitter was kindly lent by Société Nationale des Pétroles Aquitaine.

REFERENCES (Avedik *et al.*)

- Artyushkov, E. V. & Sobolev, S. F. 1981 *Mem. Am. Ass. Petrol. Geol.* (In the press.)
- Avedik, F. & Howard, D. 1979 In *Initial reports of the deep sea drilling project*, vol. 48, pp. 1015–1023. Washington, D.C.: U.S. Government Printing Office.
- Avedik, F., Renard, V., Buisine, D. & Cornic, J.-Y. 1978 *Mar. geophys. Res.* **3**, 357–379.
- Bally, A. W. & Snelson, S. 1980 In *Facts and principles of world petroleum occurrence* (ed. A. D. Miall), pp. 9–94. Canadian Society of Petroleum Geologists.
- Biju-Duval, B., Dercourt, J. & Le Pichon, X. 1977 In *Structural history of the Mediterranean basins* (ed. B. Biju-Duval & L. Montadert), pp. 143–164. Paris: Éditions Technip.
- Camus, A.-L. 1980 *Rep. Inst. fr. Pétrole*, vol. 28, no. 310. (100 pages.)
- Camus, A.-L. 1981 *Rep. Inst. fr. Pétrole*, vol. 28, no. 989. (63 pages.)
- de Charpal, O., Guennoc, P., Montadert, L. & Roberts, D. G. 1978 *Nature, Lond.* **275**, 706–711.
- Chenet, P. Y., Montadert, L., Gairaud, H. & Roberts, D. G. 1981 *Mem. Am. Ass. Petrol. Geol.* (In the press.)
- Christensen, N. I. 1966 *J. geophys. Res.* **71**, 5921–5931.
- Christensen, N. I. & Salisbury, M. H. 1975 *Rev. Geophys. Space Phys.* **13**, 57–86.
- Fenner, D. F. & Bucca, P. J. 1971 *U.S. Naval Oceanographic Office Informal Report* no. 71–13. (86 pages.)
- Fuchs, K. & Muller, G. 1971 *Geophys. Jl R. astr. Soc.* **23**, 417–433.
- Hamilton, E. L. 1978 *J. acoust. Soc. Am.* **63**, 366–377.
- Holder, A. P. & Bott, M. H. P. 1971 *Geophys. Jl R. astr. Soc.* **23**, 465–489.
- Kirk, R. E., Langford, J. J. & Whitmarsh, R. B. 1982 (In preparation.)
- Le Pichon, X. & Sibuet, J. C. 1981 *J. geophys. Res.* **86**, 3708–3720.
- Makris, J. 1977 *Geophys. Einzelschr.* **34**, 1–124.
- McKenzie, D. P. 1978 *Earth planet. Sci. Lett.* **40**, 25–32.
- Montadert, L., Roberts, D. G. *et al.* 1977 *Nature, Lond.* **268**, 305–309.
- Montadert, L., Roberts, D. G., de Charpal, O. & Guennoc, P. 1979 In *Initial reports of the Deep Sea Drilling Project*, vol. 48, pp. 1025–1060. Washington, D.C.: U.S. Government Printing Office.
- Nafe, J. & Drake, C. L. 1963 In *Physical properties of marine sediments of the sea*, vol. 3 (ed. M. N. Hill), pp. 794–815. London: Interscience.
- Profett, J. M. 1977 *Bull. geol. Soc. Am.* **88**, 247–266.
- Roberts, D. G., Masson, D. G., Montadert, L. & de Charpal, O. 1981 In *Petroleum geology of the continental shelf of northwest Europe*, pp. 455–473. London: Institute of Petroleum.
- Royden, R. & Keen, C. E. 1980 *Earth planet. Sci. Lett.* **51**, 343–361.
- Royden, L. & Sclater, J. G. 1981 *Phil. Trans. R. Soc. Lond. A* **300**, 219–222.
- Royden, L., Sclater, J. G. & Von Herzen, R. P. 1980 *Bull. Am. Ass. Petrol. Geol.* **64**, 173–187.
- Sclater, J. G. & Christie, P. A. F. 1980 *J. geophys. Res.* **85**, 3711–3739.
- Stoffa, P. L. & Buhl, P. 1979 *J. geophys. Res.* **B 84**, 7645–7660.
- Talwani, M., Worzel, J. L. & Landisman, M. 1959 *J. geophys. Res.* **64**, 49–59.
- Ziegler, P. A. 1978 *Geologie Mijnb.* **57**, 589–626.

distance/km

0

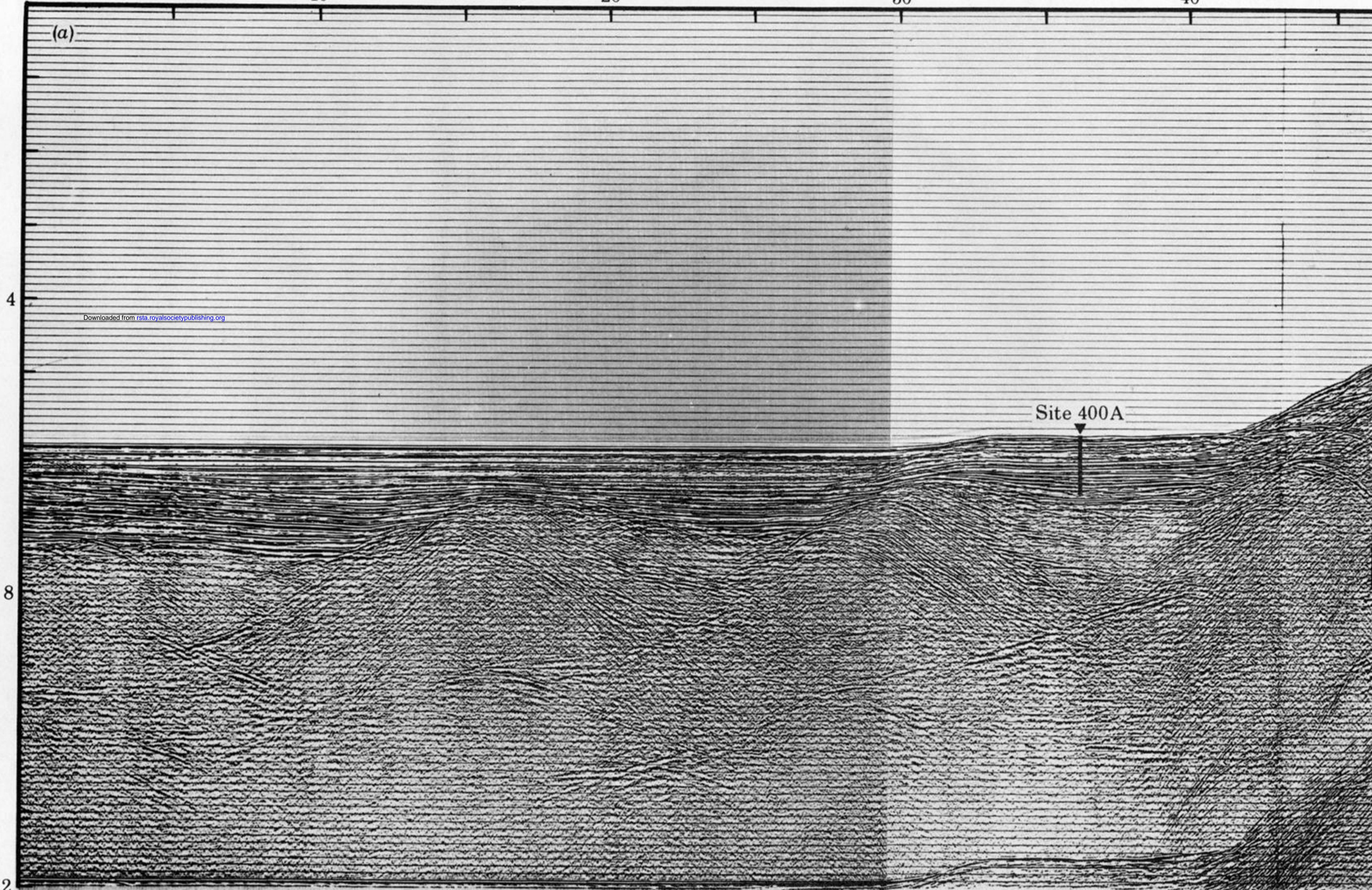
10

20

30

40

(a)



Downloaded from rsta.royalsocietypublishing.org

Site 400A

4

8

12

reduction velocity/km s⁻¹

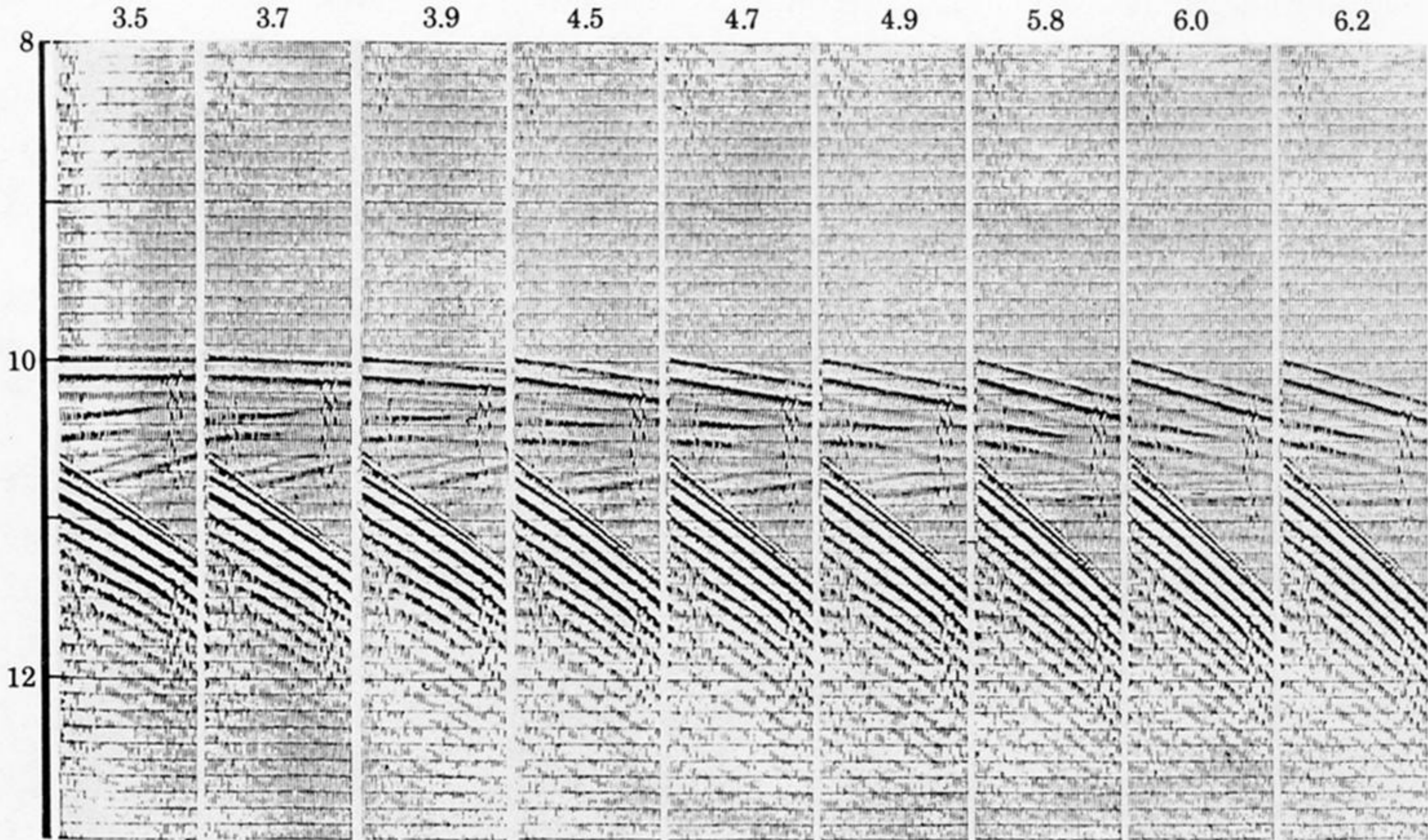


FIGURE 4. Expanding spread profile 1: examples of 48 traces per shot data displayed at different reduction velocities (from Camus 1980).

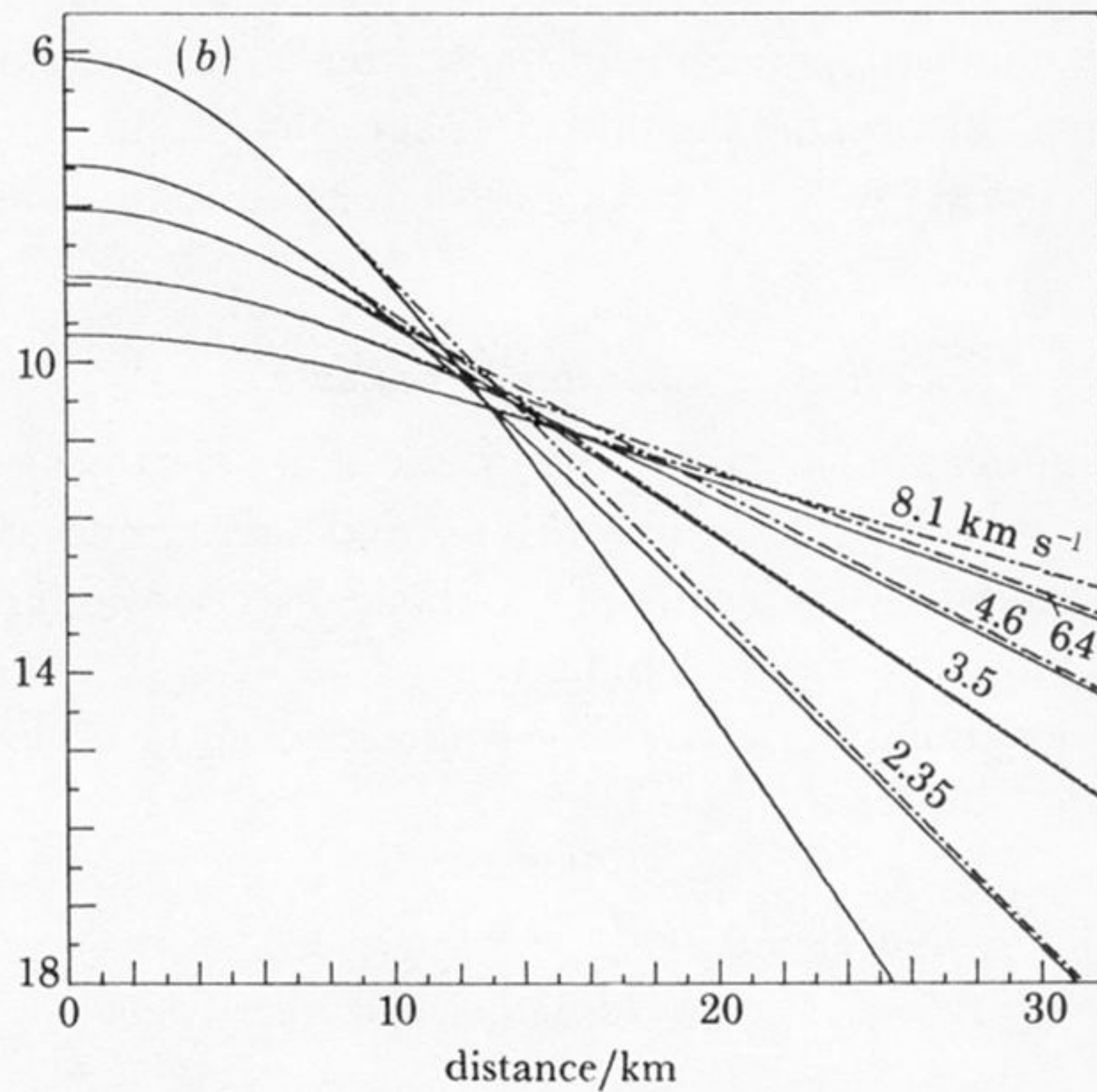
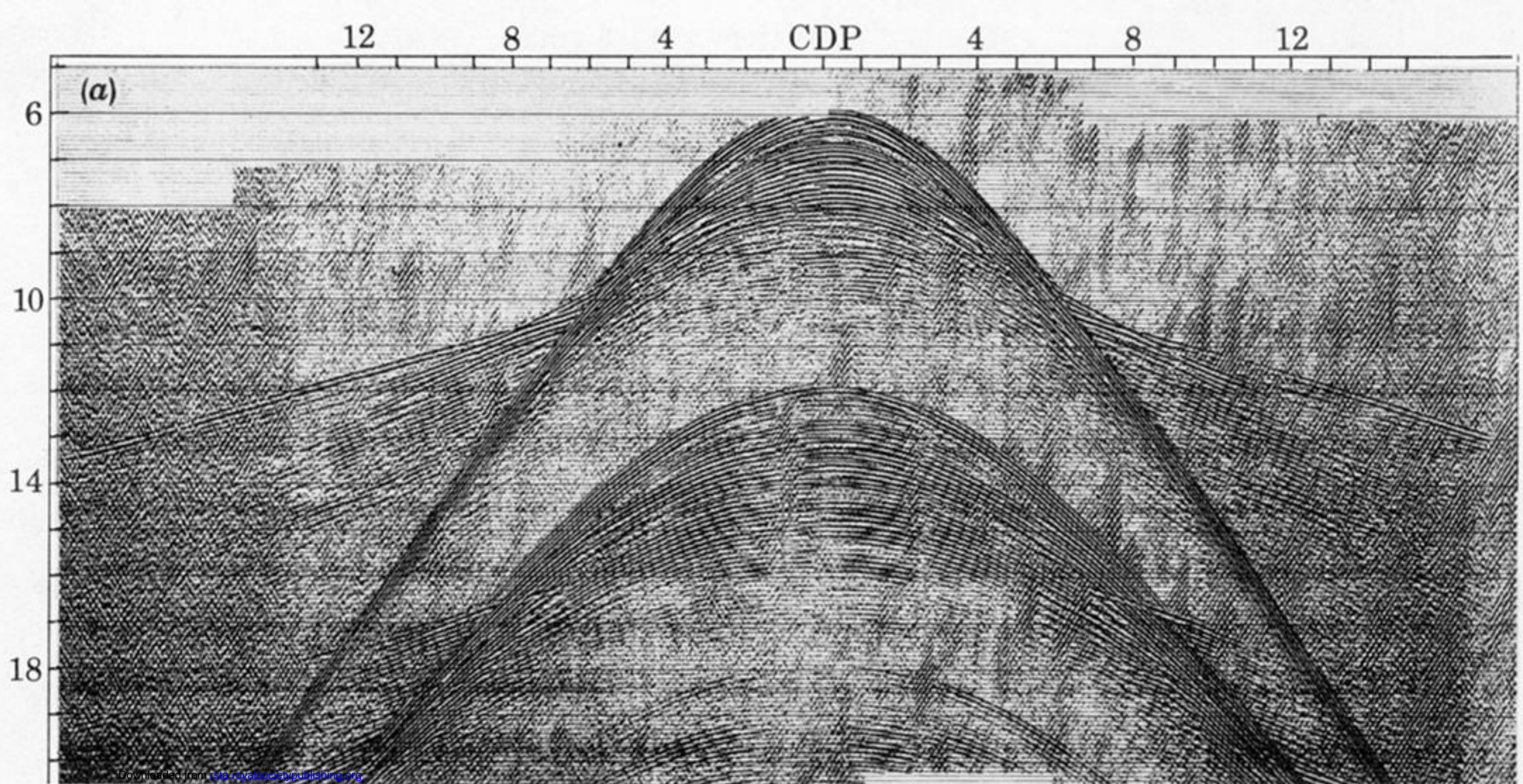


FIGURE 5. (a) Expanding spread profile 2. (b) Hodochron of expanding spread profile 2. —, Primary P-type reflexions; — · —, P-type refractions.